Regulatory Mechanisms in Biosystems

ISSN 2519-8521 (Print)
ISSN 2520-2588 (Online)
Regul. Mech. Biosyst.

Global climate change may reduce the anti-erosion regulatory capacity of vegetation cover in Ukraine's Polissya and Forest-Steppe regions

Y. Nykytiuk*, O. Kravchenko*, A. Pitsil*, V. Bambura**, D. Seredniak***

*Polissia National University, Zhytomyr, Ukraine
**M. V. Zubets Institute of Animals Breeding and Genetics National Academy of Agrarian Sciences of Ukraine, Kyiv region, Ukraine
***Institute of Plant Protection of National Academy of Agrarian Sciences of Ukraine, Kyiv, Ukraine

Article info

Received 24.11.2024
Received in revised form 17.12.2024
Accepted 15.01.2025

Polissia National University, 7 Staryi Boulevard, Zhytomyr, 10008, Ukraine.
Tel.: +38-067-448-38-48.

M. V. Zubets Institute of Animals Breeding and Genetics National Academy of Agrarian Sciences of Ukraine, Pogrebnyaka st.,ꞌ 1, Chubynske, Kyiv region, 08321, Ukraine.
Tel.: +38-067-230-02-54.

Institute of Plant Protection of National Academy of Agrarian Sciences of Ukraine, Vasylkivska st.,ꞌ 33, Kyiv, 03022, Ukraine.
Tel.: +38-067-367-07-07.

Nykytiuk, Y., Kravchenko, O., Pitsil, A., Bambura, V., & Seredniak, D. (2025). Global climate change may reduce the anti-erosion regulatory capacityof vegetation cover in Ukraine's Polissya and Forest-Steppe regions. Regulatory Mechanisms in Biosystems, 16(1), e25004. doi:10.15421/0225004

Vegetation cover is vital for landscape erosion resistance, landform shaping, soil fertility, and water quality preservation. The cover management factor (C-factor) is commonly used to assess land use and management impacts. This study analyzes the spatial and temporal variability of the C-factor in Polissya and the forest-steppe of Ukraine, forecasting its changes in the coming decades due to climate change. NDVI data throughout the year were used to calculate the C-factor. NDVI rises from spring to early summer, peaking in June, then declines through summer and autumn into winter. Different landscape covers exhibit unique NDVI patterns. Agricultural land shows decreased NDVI in late summer, correlating with harvest time, while winter NDVI values are low. Broadleaf forests maintain stable summer NDVI, coniferous forests show consistent levels, and mixed forests fall between the two. Meadow ecosystems see a significant NDVI increase in April. NDVI growth in floodplain vegetation is slower in the first half of the year, reaching its annual maximum later than other vegetation types. Artificial cover types have lower NDVI values, and aquatic ecosystems exhibit low NDVI and slower dynamics. The study area's C-factor is 0.19 ± 0.11, with bioclimatic variables explaining 77% of its variation. Mean annual temperature and mean diurnal range are significant predictors of C-factor increases, while higher isothermality reduces C-factor values. Monthly temperature amplitude is a sensitive predictor, and the C-factor is responsive to monthly or quarterly precipitation but not to annual precipitation. The resulting regression model was developed based on a wide range of environmental conditions, aligning with the predicted time scale of climate change. This model forecasts a steady increase in the C-factor over the coming decades. Our findings support projections that soil erosion rates will rise by the end of the 21st century due to climate change, which reduces soil moisture and increases precipitation intensity. Global warming and changing precipitation patterns are expected to decrease vegetation cover density, reducing its protective capacity against soil erosion. The study region will experience varying impacts of climate change, with the greatest erosion control risks in the east and a critical zone extending southwest over time. This trend underscores the urgent need for soil erosion control, particularly in the northeast and center, while the southwest will face challenges later. Addressing global climate change requires a unified response, as regional measures alone cannot influence the global situation. Effective land use management is essential to mitigate the negative effects of climate change on soil erosion. Projected bioclimatic values enabled scenarios for potential spatial changes in the C-factor over time. This forecast provides insights for agronomists and environmentalists, forming a basis for effective erosion control measures and optimizing environmental protection efforts.

Keywords: climate change; spatial pattern; temporal dynamic; landscape; soil cover.

Introduction

Soil erosion is a major global issue causing land degradation (Luvai et al., 2022). Water erosion, a natural process influenced by human activities, affects landform development (Pimentel et al., 1995). Erosion rates on agricultural land impact sustainability and have economic consequences (Doran, 2002). Eroded soil contributes materials to water bodies, increasing sedimentation and degrading water quality (Wang et al., 2023). Agricultural technologies and land management practices are essential for controlling soil erosion. Vegetation significantly controls soil erosion dynamics (Zelenova et al., 2024), with water erosion rates decreasing exponentially as vegetation cover increases. This reduction in soil loss is due to the combined effects of roots and canopy (Gyssels et al., 2005). Soil erosion is also affected by land use and management factors, such as crop type and tillage practices (Kuhwald et al., 2022). Zero tillage and cross-slope tillage are effective methods for preventing erosion in agriculture (Kisic et al., 2017). Monitoring soil erosion risk is vital for conservation (Kunakh et al., 2023). Geographic Information Systems (GIS) and remote sensing are effective tools for assessing natural resources (Sharma et al., 2024).

The cover management factor (C-factor) is used to assess the impacts of land use and management on soil erosion (Ebabu et al., 2022). The RUSLE model integrates geographic information systems (GIS) and remote sensing (Luvai et al., 2022). The C-factor is one of the five factors used to assess soil erosion risk in the Universal Soil Loss Equation (USLE) and its revised version (RUSLE) (Carollo et al., 2024). The C-factor, a key component of the Universal Soil Loss Equation (USLE) and RUSLE, compares long-term soil loss from cropland to that from a net fallow area on a 22 m slope with a 9% gradient. Initially determined through long-term erosion experiments, the C-factor's accuracy is influenced by seasonal variations in vegetation density. The RUSLE model considers factors such as previous crops, vegetation cover, and soil moisture in its erosion estimates. The C-factor is essential for policy and land use decisions, as it identifies manageable conditions for reducing erosion (Renard et al., 1991). It also reflects how land cover and management practices affect soil loss compared to pure fallow land (Kinnell, 2010).

The Normalized Difference Vegetation Index (NDVI) is used to map vegetation parameters and estimate C-factors at large scales (Suriyaprasita & Shrestha, 2008). Remote sensing imagery has become a common method for creating C-factor maps based on vegetation indices, such as the Normalised Difference Vegetation Index (NDVI), which has become a prevalent methodology (Alexandridis et al., 2015). Evidence shows that combining stratified coverage indices with remote sensing indices improves C-factor estimation (Feng et al.,

2018). This data makes it possible to create monthly C-factor maps, mean values for the growing season, and annual means. C-factor values from remote sensing indicate temporal variability for crops (Pechanec et al., 2018). Understanding the dynamics of erosion factors helps agronomists implement targeted control measures, reducing mitigation costs (Schmidt et al., 2018). The NDVI method effectively reflects vegetation cover and captures spatial and temporal changes (Alexandridis et al., 2015).

Vegetation cover is essential for erosion resistance, soil fertility, and provides a dynamic balance in the formation of landforms, maintaining soil fertility and preserving water quality (Mykhailyuk et al., 2023). While modeling the spatial variability of the C-factor poses challenges, forecasting its variability over time due to global climate change is still needed. This study aims to assess the C-factor's spatial and temporal variability under the conditions of global climate change and develop a forecast for the coming decades.

Materials and methods

The study examined the Polissya and Forest-Steppe regions of Ukraine (Zymaroieva et al., 2019). C-factors are essential for crop management, reflecting the effect of vegetation cover on soil erosion (Renard et al., 1997). The C-factor varies by season and crop production system, influenced by precipitation, agricultural practices, and crop type. It ranges from nearly zero for well-protected cover to 1 for barren areas. Consequently, its impact on soil erosion may be minimal in areas with a high percentage of forest and plantation crops.

NDVI (Normalized Difference Vegetation Index) measures vegetation condition and vitality, indicating green vegetation and photosynthetic activity. Vegetation suggests limited exposure to raindrops, which can initiate soil erosion processes. Detecting vegetation typically requires remote sensing techniques for monitoring and analyzing ecosystems. Vegetation cover is a key indicator of soil erosion, distinguishing between vegetation and soil distribution based on reflectance patterns (Rahman et al., 2009). The NDVI is given below as:

$$NDVI = \frac{(NIR - RED)}{NIR + RED},$$

where NIR is the near-infrared value and RED is the red band value, which reflects the proportion of absorbed photosynthetic active radiation. The NDVI values obtained for different locations in the study area are used to produce an NDVI map that reflects land cover management. The values for NDVI range from –1.0 to 1.0, where higher values represent green vegetation and lower values represent normal soil or water surface materials. The C factor can be estimated by applying the following ratio (Zhou et al., 2008; Kouli et al., 2009):

$$C = \exp\left(-a \times \frac{NDVI}{b - NDVI}\right),$$

where C is the calculated crop management coefficient; NDVI is the normalised differential vegetation index; α and β are two scaling factors. The values for the two scaling factors α and β are 2 and 1 respectively (Van der Knijff et al., 2000). Terra-based vegetation indices (MODIS) data (MOD13Q1) version 6 are generated every 16 days at a spatial resolution of 250 m as a level 3 product. The MODIS-derived NDVI of the study area was calculated for each month of the year and used to determine the C factor.

Results

During the growing season, NDVI increases from spring to early summer. In June, this indicator reaches its maximum, in the summer months NDVI slowly decreases, after which it sharply decreases in autumn and until the beginning of winter. Different types of landscape cover have certain differences from the general trend. Agricultural land is characterised by a sharp decline in NDVI in the second half of summer, which corresponds to the harvest time. Also, in winter, NDVI has very low values for agricultural areas. Broadleaf forests are characterised by a plateau in NDVI values in summer. Coniferous forests are characterised by levelled NDVI values throughout the season. Naturally, mixed forests occupy a transitional position between broadleaved and coniferous forests in terms of NDVI dynamics over time. Meadow ecosystems are characterised by a sharp increase in NDVI in April. Floodplain vegetation demonstrates a slower growth rate of NDVI in the first half of the year and reaches its annual maximum somewhat later than other vegetation types. Artificial cover types have generally lower NDVI values. Aquatic ecosystems also have low NDVI values and slower annual dynamics.

The C-factor calculated from the NDVI values is 0.19 ± 0.11. The highest C-factor values were for Bare areas and Artificial areas (0.29 ± 0.12 and 0.26 ± 0.07 respectively). Also, this index was high for Sparse vegetation and Croplands (0.25 ± 0.08 and 0.23 ± 0.07, respectively). Mosaic landscape complexes with Croplands had a slightly lower C-factor value (0.21 ± 0.07). Broadleaf forests had a C-factor value of 0.14 ± 0.05, and communities with coniferous plant species had this indicator at the level of 0.09 ± 0.05. Shrub and meadow communities had a C-factor value of 0.13 ± 0.05. In space, the lowest C-factor values were typical for the northern and southeastern parts of the region, and the highest - for the southern and eastern parts (Fig. 1).

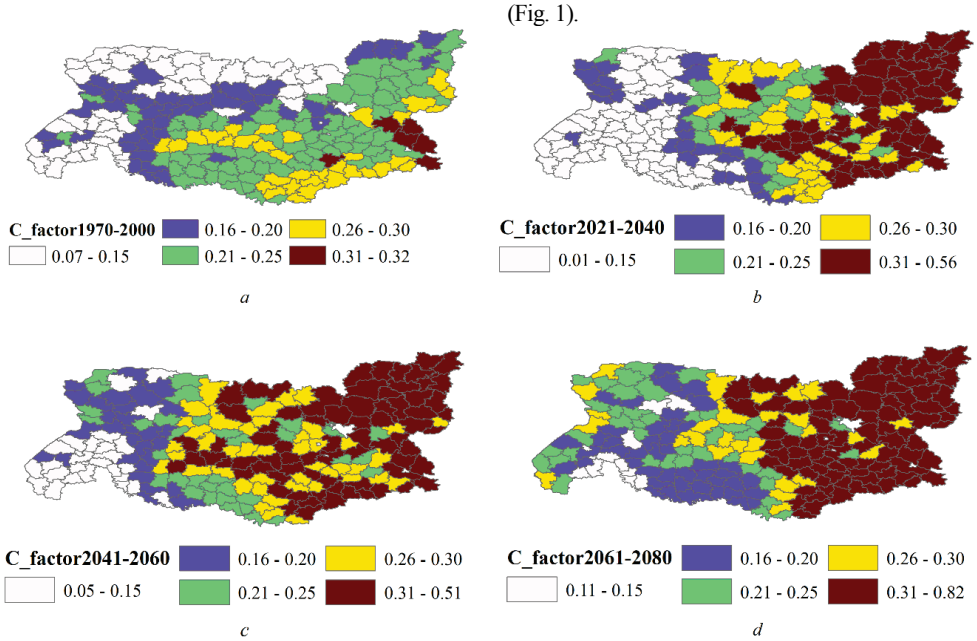

Fig. 1. Spatial variability of the vegetation cover erosion control factor (C-factor) and its forecast over time: *a* is the variability of the indicator for the period 1970–2000; *b* is the forecast of the indicator's variability for the period 2021–2040; *c* is the forecast of the indicator's variability for the period 2041–2060; *d* is the forecast of the indicator's variability for the period 2061–2080

Bioclimatic variables were able to explain 77% of the variation in the C-factor (Table 1). An increase in mean annual temperature and mean diurnal range were statistically significant predictors of an increase in the C-factor. On the contrary, an increase in isothermality indicates a decrease in C-factor values. Amplitude monthly temperatures are also sensitive predictors of C-factor changes. The C-factor was not sensitive to annual precipitation, but was sensitive to precipitation by month or quarter. Using the predicted values of the bioclimatic variables for the resulting model, we developed scenarios of spatial changes in the C-factor for different periods of the future.

The forecast indicates a monotonous increase in the C-factor until 2080 as a response to global climate change (Figure 2). In the period 2021–2040 the C-factor will increase by 13.7% compared to 1970–2000 ($t = 3.4$, $P < 0.001$). The growth will be most pronounced in the east and centre of the region. In the period 2041–2060, the growth will be 13.2% compared to the previous one ($t = 3.1$, $P = 0.002$). The growth area will mostly cover the east, but will also extend to the central part of the region. In the period 2061–2080, growth will be 10.3% ($t = 2.6$, $P = 0.01$). The growth zone will extend to the east and centre of the region. Differential indicators are more sensitive to determine the main directions of the spatial and temporal dynamics of the C-factor (Fig. 3). In the period 2021–2040, the C-factor will increase in the northeast of the region, while in the southwest there will be a downward trend in this indicator. In the next time period, the area of C-factor decline will be located in the east of the region, and the area of growth will be located in the southwest of the region. In the period 2061–2080, the zone of C-factor increase will be located on the periphery of the region, and the zone of C-factor decrease will be in the centre of the region.

The dynamics of the C-factor depends on both climate trends and the type of landscape cover (Table 2). Soil properties will contribute to the C-factor dynamics in different ways at different time stages. The role of soil organic matter will only become apparent in the period 2061–2080, while the direction of influence of the content of particle size fractions will change in 2021–2040 and 2041–2060. The contribution of different land cover types is also dynamic, and their direction of influence changes over time.

Table 1

Multiple regression analysis of the dependence of the factor of erosion control of vegetation cover (C-factor) on bioclimatic variables ($R_{adj}^2 = 0.77$, $F = 40.8$, $P < 0.001$)

Bioclimatic variable	Beta regression coefficient ± standard error	Regression coefficient ± standard error	*t*(186)	*P*–value
Intercept	–	0.20 ± 0.02	8.08	<0.001
Annual Mean Temperature (Bio_1)	15.09 ± 2.41	0.49 ± 0.08	6.25	<0.001
Mean diurnal range (Bio_2)	13.71 ± 1.77	0.37 ± 0.05	7.73	<0.001
Isothermality (Bio_3)	–12.29 ± 1.57	–0.10 ± 0.01	–7.83	<0.001
Temperature seasonality (Bio_4)	–1.10 ± 5.75	0.00 ± 0.00	–0.19	0.85
Max temperature of warmest month (Bio_5)	–12.68 ± 3.66	–0.12 ± 0.04	–3.46	0.001
Min temperature of coldest month (Bio_6)	7.23 ± 0.67	0.19 ± 0.02	10.72	<0.001
Temperature annual range (Bio_7)	0.02 ± 0.12	0.01 ± 0.03	0.19	0.85
Mean temperature of wettest quarter (Bio_8)	–1.34 ± 0.92	–0.02 ± 0.01	–1.46	0.15
Mean temperature of driest quarter (Bio_9)	0.42 ± 0.18	0.03 ± 0.01	2.34	0.02
Mean temperature of warmest quarter (Bio_10)	–6.78 ± 7.98	–0.09 ± 0.10	–0.85	0.39
Mean temperature of coldest quarter (Bio_11)	–8.12 ± 1.58	–0.40 ± 0.08	–5.14	<0.001
Annual precipitation (Bio_12)	0.38 ± 2.63	0.00 ± 0.00	0.14	0.89
Precipitation of wettest month (Bio_13)	–5.81 ± 1.28	–0.01 ± 0.00	–4.55	<0.001
Precipitation of driest month (Bio_14)	3.13 ± 0.82	0.02 ± 0.01	3.80	<0.001
Precipitation seasonality (Bio_15)	4.31 ± 1.09	0.03 ± 0.01	3.94	<0.001
Precipitation of wettest quarter (Bio_16)	–22.44 ± 4.12	–0.02 ± 0.00	–5.45	<0.001
Precipitation of driest quarter (Bio_17)	4.67 ± 1.74	0.01 ± 0.00	2.68	0.008
Precipitation of warmest quarter (Bio_18)	23.18 ± 3.79	0.02 ± 0.00	6.11	<0.001
Precipitation of coldest quarter (Bio_19)	–2.10 ± 1.23	0.00 ± 0.00	–1.71	0.09

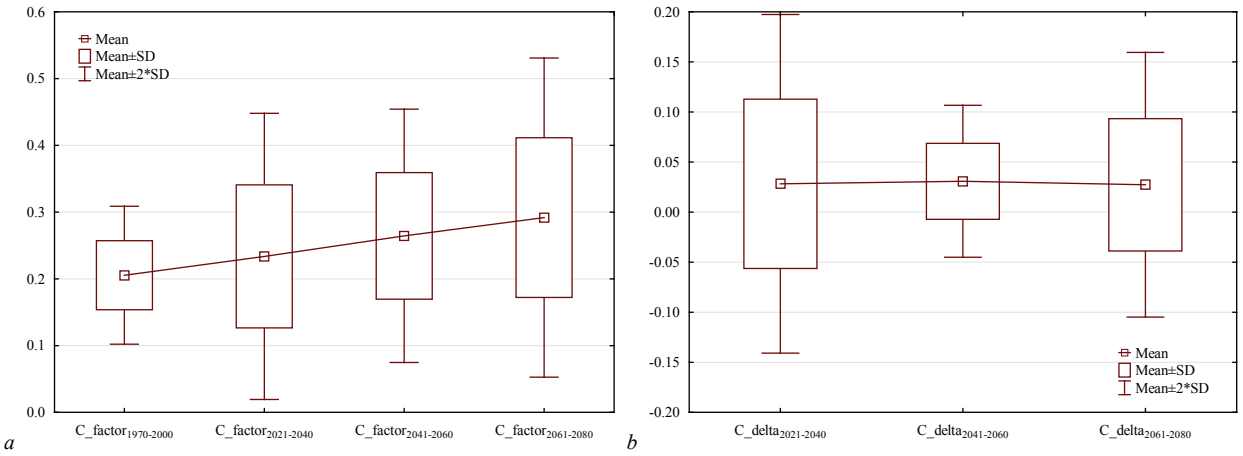

a *b*

Fig. 2. Variability of the vegetation cover erosion control factor (C-factor) and its forecast over time: a is an estimate for the period 1970–2000 and a forecast for the periods 2021–2040, 2041–2060, and 2061–2080; b is a forecast of the increase in the indicator for successive time periods

Discussion

Vegetation density is the most important driver of C-factor variability (Pinson & AuBuchon, 2023). NDVI is a sensitive indicator of vegetation density, and modern remote sensing technologies allow data to be obtained with sufficient spatial and temporal resolution (Martinez & Labib, 2023). The seasonal dynamics of vegetation density determines the ability of plants to counteract soil erosion (Alexandridis et al., 2015).

We found that landscape cover types have specific patterns of seasonal variability in NDVI. The NDVI value is also influenced by the dynamics of climatic conditions, soil moisture content, and ground water level. Human activity has the strongest impact on NDVI. Land use change caused by human activity leads to a decrease in

NDVI (Chang et al., 2022). The general temporal trend of NDVI variability follows a sinusoidal curve with a minimum corresponding to the winter period and a maximum corresponding to the summer period. The differences between the types of landscape cover lie in the average level of NDVI throughout the year, the maximum level in summer and the minimum level in winter, and in the dynamics of reaching maximum levels or in the dynamics of NDVI decline after the seasonal maximum. It is obvious that the protective potential of vegetation cover against soil erosion is greater the denser the vegetation cover and the longer the dense cover is maintained (Ruiz-Colmenero et al., 2013).

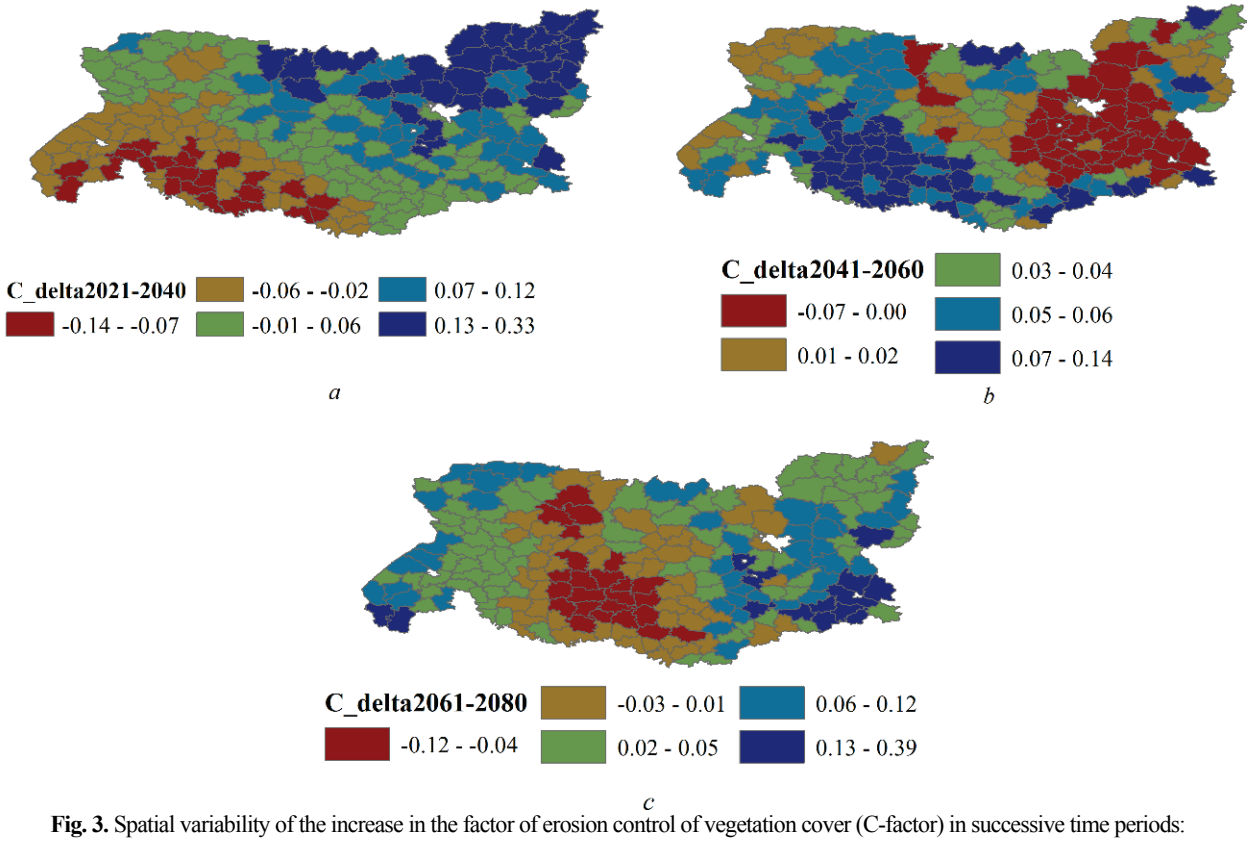

Fig. 3. Spatial variability of the increase in the factor of erosion control of vegetation cover (C-factor) in successive time periods: *a* is the variability of the indicator for the period 1970–2000; *b* is the forecast of the indicator's variability for the period 2021–2040; *c* is the forecast of the indicator's variability for the period 2041–2060; *d* is the forecast of the indicator's variability for the period 2061–2080

Table 2

Correlation of soil properties, landscape cover types and the relief erosion factor (LS) with increases in the erosion control factor of vegetation cover (C-factor) in successive time periods (correlation coefficients are shown, which are statistically significant for $P < 0.05$)

Variable	Successive periods		
	from 1970–2000 to 2021–2040	from 2021–2040 to 2041–2060	from 1970–2000 to 2021–2040
OM	–	–	0.18
Clay	–0.48	0.24	–
Sand	0.43	–0.23	–
Silt	–0.33	0.20	–
Rainfed croplands	–0.38	0.19	–0.18
Mosaic Croplands/Vegetation	0.14	–	–0.18
Mosaic Vegetation/Croplands	–0.14	–	–
Closed broadleaved deciduous forest	–	–	–
Closed needleleaved evergreen forest	0.35	–	–
Open needleleaved deciduous or evergreen forest	0.41	–0.15	–
Closed to open mixed broadleaved and needleleaved forest	0.34	–	–
Mosaic Grassland/Forest–Shrubland	–0.36	–	–
Closed to open grassland	–0.24	–	0.17
Sparse vegetation	–0.15	–	–
Closed to open vegetation regularly flooded	0.16	–	–0.01
Artificial areas	–	–	–
Water bodies	0.21	–0.18	0.29

Our results support the generalisation that vegetation cover structure affects runoff formation and soil erosion under the influence of precipitation. Soil loss is more easily regulated by the proportion and spatial structure of vegetation cover than by runoff. The potential of vegetation cover to regulate soil loss responds positively to precipitation depth and intensity (Tang et al., 2021). Forest ecosystems have the most extensive vegetation cover (Yakovenko et al., 2023). Coniferous forests have the most levelled temporal dynamics of NDVI. This means that the differences in NDVI between winter and summer for this land cover type are the smallest among all the land cover types studied. The peculiarity of broadleaf forests is that they reach the summer NDVI maximum earlier than coniferous forests, and the plateau of summer NDVI values lasts longer. The maximum NDVI values of agricultural land are practically the same as those of other vegetation types. In addition, agricultural landscapes are characterised by the presence of two local NDVI maxima: summer and autumn. Obviously, the autumn one corresponds to the development of winter crops or the development of weeds after harvesting. The rapid increa-

se in NDVI in spring on agricultural land is due to the specifics of cultivated plants that grow in artificially created best conditions for this type of plant, so their growth rate is quite high. In the second half of the summer, a sharp decrease in NDVI is the result of ripening and harvesting.

Information on the dynamics of NDVI over the course of the year was used to calculate the C-factor. The forest has the highest potential for soil protection from water erosion, while agricultural land and anthropogenic land have the lowest potential. The estimated value of the C-factor is 0.19 ± 0.11, which is in the range between the estimates for arid (0.26) and humid (0.15) climates (Ebabu et al., 2022). The greatest C-factor values were found for artificial or open areas, as well as for areas with sparse vegetation cover or agricultural areas. These results are in line with findings that the global average C-factor varies by one order of magnitude from cropland (0.34) to forest (0.03) (Ebabu et al., 2022). Among the major crops, the average C-factor is highest for maize (0.42) and potatoes (0.40) (Ebabu et al., 2022). It should be noted that the average C-factor in Europe is 0.1, with extremely high variability. Forests have the lowest average C-factor (0.001), while cropland and sparse forests have the highest (0.23 and 0.27, respectively) (Panagos et al., 2015).

The spatial patterns of landscape diversity variability explain the changes in the C-factor. The density of forest ecosystems in the region is highest in the north and east, which is why the C-factor is lowest in these areas. Towards the southeast, the C-factor tends to increase. The increase in agricultural land, as well as anthropogenic surfaces, is likely to be the reason for this trend (Zhukov et al., 2022). The spatial variability of the C-factor also depends on the influence of climatic factors. A combination of bioclimatic variables can explain a significant component of C-factor variability in space. An increase in the average annual temperature contributes to an increase in the C-factor. Obviously, higher temperatures are favourable for agricultural development by reducing the area covered by forest ecosystems, which reduces the protective capacity of vegetation cover to withstand erosion (Kunakh et al., 2020). Higher temperatures also contribute to higher levels of water evaporation from the soil surface (Kerridge et al., 2013), which can reduce the maximum density of vegetation cover. The temperature range as an indicator of climate continentality contributes to the growth of the C-factor. Temperature variability is also a significant stress factor, and its increase negatively affects the density of vegetation cover (Ridolfi et al., 2000). At a certain level of average annual temperature, an increase in the maximum temperature of the warmest month and the minimum temperature of the coldest month contribute to a decrease in the C-factor. This result can be interpreted as an increase in vegetation density due to additional heat supply.

The precipitation of the driest month and the seasonality of precipitation contribute to the growth of the C-factor, while the precipitation of the wettest month reduces this indicator. It is also worth noting the impact on the C-factor of other bioclimatic variables that characterise the seasonal redistribution of precipitation. This indicates that not only annual precipitation is important for the formation of dense vegetation cover (Kunakh et al., 2024). A decrease in vegetation cover is one of the main factors leading to soil erosion (Schmidt et al., 2018). Of greater importance is a certain pattern of annual precipitation distribution to which plant species adapt. It is this pattern that is sensitive to global climate change, which can affect the formation of vegetation cover and its ability to counteract soil erosion.

The resulting regression model was created on the basis of a significant range of environmental conditions, the spatial scale of variability of which is commensurate with the time scale of climate change predicted for the coming decades. This provides grounds for applying the model to forecast changes in the C-factor in the context of global climate change. The forecast indicates that the C-factor will grow monotonically in the coming decades. Our results are in line with findings that the projected rate of soil erosion by the end of the 21st century will accelerate as climate change reduces soil moisture while increasing precipitation intensity (Pinson & AuBuchon, 2023). Obviously, global warming and variability in precipitation patterns will be the mechanisms through which vegetation density may decrease, and, consequently, the protective capacity to counter soil erosion will decrease (Kunakh & Zhukov, 2024). The study region covers a large area within which global climate change will not be uniform. Therefore, different directions and intensity of changes are predicted. The greatest risks of erosion control capacity decline can be expected in the east of the region. The critical zone will also extend to the southwest of the region over time. From a practical point of view, this trend makes the problem of soil erosion control acute throughout the region. On the other hand, the forecast makes it possible to prioritise the goals for reducing erosion risks. Obviously, the problem is most acute in the northeast and centre of the region. The south-west will become a problem a little later. Global climate change requires a consolidated response from humanity as a whole, and in this sense, regional measures will not be able to influence the global situation (Lisovets et al., 2024). The structure of land use types is the main area of management that can minimise the negative effects of global climate change on soil erosion (Molozhon et al., 2023). It is also worth noting the effectiveness of modern farming technologies to combat soil erosion. Conservation management practices such as reduced or no tillage, the use of cover crops or crop residues reduce the C-factor by an average of 19.1% on arable land (Panagos et al., 2015). Land-use changes such as reforestation and reduction of arable land to the optimum level will have a positive anti-erosion effect. Encouraging the cultivation of more renewable energy crops will help protect soils.

Conclusion

The C-factor score for the study area is 0.19 ± 0.11 and varies by landscape type. The highest C-factor values were observed in croplands, bare areas, and artificial areas. The lowest C-factor values were observed in coniferous and broadleaf forests. The dynamics of the C-factor are contingent upon both climatic trends and the specific type of landscape cover. The analysis revealed that bioclimatic variables were able to explain 77% of the observed variation in the C-factor. The NDVI is a sensitive indicator of vegetation density, and the advent of modern remote sensing technologies has enabled the acquisition of data with sufficient spatial and temporal resolution. The differences between landscape cover types are evident in the average level of NDVI throughout the year, the maximum level in summer and the minimum level in winter, and in the dynamics of reaching maximum levels or in the dynamics of NDVI decline after the seasonal maximum. The dynamics of the NDVI throughout the year formed the basis for calculating the C-factor. The forecast indicates a gradual and uninterrupted increase in the C-factor until 2080, which can be attributed to the effects of global climate change. During the period between 2021 and 2040, the C-factor is expected to increase in the north-eastern region, while a downward trend is anticipated in the south-western region. Subsequently, the area of decline in the C-factor will be located in the eastern region, while the area of growth will be located in the southwestern region. In the period between 2061 and 2080, the zone of C-factor increase will be located on the periphery of the region, while the zone of C-factor decrease will be situated in the centre of the region. The resulting forecast of the spatial and temporal dynamics of the C-factor provides valuable information for agronomists and environmentalists. This forecast serves as the foundation for the development of effective erosion control measures in specific areas and at designated times, thereby ensuring the optimal distribution of erosion mitigation efforts and conservation measures.

References

Alexandridis, T. K., Sotiropoulou, A. M., Bilas, G., Karapetsas, N., & Silleos, N. G. (2015). The effects of seasonality in estimating the C-factor of soil erosion studies. Land Degradation and Development, 26(6), 596–603.

Carollo, F. G., Serio, M. A., Pampalone, V., & Ferro, V. (2024). The unit plot of the universal soil loss equation (USLE): Myth or reality? Journal of Hydrology, 632, 130880.

Chang, J., Gong, L., Zeng, F., Xue, J., Mao, D., Cao, Y., Mu, G., & Wang, S. (2022). Using hydro-climate elasticity estimator and geographical detector method to quantify the individual and interactive impacts on NDVI in oa-

sis-desert ecotone. Stochastic Environmental Research and Risk Assessment, 36(10), 3131–3148.
Doran, J. W. (2002). Soil health and global sustainability: Translating science into practice. Agriculture, Ecosystems and Environment, 88(2), 119–127.
Ebabu, K., Tsunekawa, A., Haregeweyn, N., Tsubo, M., Adgo, E., Fenta, A. A., Meshesha, D. T., Berihun, M. L., Sultan, D., Vanmaercke, M., Panagos, P., Borrelli, P., Langendoen, E. J., & Poesen, J. (2022). Global analysis of cover management and support practice factors that control soil erosion and conservation. International Soil and Water Conservation Research, 10(2), 161–176.
Feng, Q., Zhao, W., Ding, J., Fang, X., & Zhang, X. (2018). Estimation of the cover and management factor based on stratified coverage and remote sensing indices: A case study in the Loess Plateau of China. Journal of Soils and Sediments, 18(3), 775–790.
Gyssels, G., Poesen, J., Bochet, E., & Li, Y. (2005). Impact of plant roots on the resistance of soils to erosion by water: A review. Progress in Physical Geography: Earth and Environment, 29(2), 189–217.
Kerridge, B. L., Hornbuckle, J. W., Christen, E. W., & Faulkner, R. D. (2013). Using soil surface temperature to assess soil evaporation in a drip irrigated vineyard. Agricultural Water Management, 116, 128–141.
Kinnell, P. I. A. (2010). Event soil loss, runoff and the Universal Soil Loss Equation family of models: A review. Journal of Hydrology, 385, 384–397.
Kisic, I., Bogunovic, I., Birkás, M., Jurisic, A., & Spalevic, V. (2017). The role of tillage and crops on a soil loss of an arable Stagnic Luvisol. Archives of Agronomy and Soil Science, 63(3), 403–413.
Kouli, M., Soupios, P., & Vallianatos, F. (2009). Soil erosion prediction using the Revised Universal Soil Loss Equation (RUSLE) in a GIS framework, Chania, Northwestern Crete, Greece. Environmental Geology, 57(3), 483–497.
Kuhwald, M., Busche, F., Saggau, P., & Duttmann, R. (2022). Is soil loss due to crop harvesting the most disregarded soil erosion process? A review of harvest erosion. Soil and Tillage Research, 215, 105213.
Kunakh, O. M., Volkova, A. M., Tutova, G. F., & Zhukov, O. V. (2023). Diversity of diversity indices: Which diversity measure is better? Biosystems Diversity, 31(2), 131–146.
Kunakh, O. M., Yorkina, N. V., Zhukov, O. V., Turovtseva, N. M., Bredikhina, Y. L., & Logvina-Byk, T. A. (2020). Recreation and terrain effect on the spatial variation of the apparent soil electrical conductivity in an urban park. Biosystems Diversity, 28(1), 3–8.
Kunakh, O., & Zhukov, O. (2024). Spatial organization of the soil macrofauna community of an oak forest in the steppe zone of Ukraine. Studia Biologica, 18(3), 99–120.
Kunakh, O., Ivanko, I., Holoborodko, K., & Zhukov, O. (2024). A spontaneous spread of black locust (*Robinia pseudoacacia* L.): The importance of seed and vegetative reproduction. Folia Oecologica, 51(2), 120–135.
Lisovets, O., Khrystov, O., Kunakh, O., & Zhukov, O. (2024). Application of hemeroby and naturalness indicators for monitoring the aquatic macrophyte communities in protected areas. Biosystems Diversity, 32(2), 270–277.
Luvai, A., Obiero, J., & Omuto, C. (2022). Soil loss assessment using the revised universal soil loss equation (RUSLE) model. Applied and Environmental Soil Science, 2022(5), 2122554.
Martinez, A. de la I., & Labib, S. M. (2023). Demystifying normalized difference vegetation index (NDVI) for greenness exposure assessments and policy interventions in urban greening. Environmental Research, 220, 115155.
Molozhon, K. O., Lisovets, O. I., Kunakh, O. M., & Zhukov, O. V. (2023). Increased soil penetration resistance drives degrees of hemeroby in vegetation of urban parks. Biosystems Diversity, 31(4), 411–419.
Panagos, P., Borrelli, P., Meusburger, K., Alewell, C., Lugato, E., & Montanarella, L. (2015). Estimating the soil erosion cover-management factor at the European scale. Land Use Policy, 48, 38–50.
Pechanec, V., Mráz, A., Benc, A., & Cudlín, P. (2018). Analysis of spatiotemporal variability of C-factor derived from remote sensing data. Journal of Applied Remote Sensing, 12(1), 16022.
Pimentel, D., Harvey, C., Resosudarmo, P., Sinclair, K., Kurz, D., McNair, M., Crist, S., Shpritz, L., Fitton, L., Saffouri, R., & Blair, R. (1995). Environmental and economic costs of soil erosion and conservation benefits. Science, 267(5201), 1117–1123.
Pinson, A. O., & AuBuchon, J. S. (2023). A new method for calculating C factor when projecting future soil loss using the Revised Universal soil loss equation (RUSLE) in semi-arid environments. Catena, 226, 107067.
Rahman, E. L., Abd, M. A., Ali, R. R., Hussain, M. A., & El-Semey, M. A. (2009). Remote sensing and GIS based physiography and soils mapping of the Idku-Brullus Area, North Delta, Egypt. Egyptian Journal of Soil Science, 49(3), 409–432.
Renard, K. G., Foster, G. R., Weesies, G. A., & Porter, J. P. (1991). RUSLE: Revised Universal Soil Loss Equation. Soil and Water Conservation, 46, 30–33.
Renard, K., Foster, G., Weesies, G., McCool, D., & Yoder, D. (1997). Predicting soil erosion by water: A guide to conservation planning with the Revised Universal Soil Loss Equation (RUSLE). US Government Printing Office.
Ridolfi, L., D'Odorico, P., Porporato, A., & Rodriguez-Iturbe, I. (2000). Impact of climate variability on the vegetation water stress. Journal of Geophysical Research: Atmospheres, 105(D14), 18013–18025.
Ruiz-Colmenero, M., Bienes, R., Eldridge, D. J., & Marques, M. J. (2013). Vegetation cover reduces erosion and enhances soil organic carbon in a vineyard in the Central Spain. Catena, 104, 153–160.
Schmidt, S., Alewell, C., & Meusburger, K. (2018). Mapping spatio-temporal dynamics of the cover and management factor (C-factor) for grasslands in Switzerland. Remote Sensing of Environment, 211, 89–104.
Sharma, S., Beslity, J. O., Rustad, L., Shelby, L. J., Manos, P. T., Khanal, P., Reinmann, A. B., & Khanal, C. (2024). Remote sensing and GIS in natural resource management: Comparing tools and emphasizing the importance of *in-situ* data. Remote Sensing, 16(22), 4161.
Suriyaprasita, M., & Shrestha, D. P. (2008). Deriving land use and canopy cover factor from remote sensing and field data in inaccessible mountainous terrain for use in soil erosion modeling. The International Archives of the Photogrammetry, Remote Sensing and Spatial Information Sciences, 37, 1747–1750.
Tang, C., Liu, Y., Li, Z., Guo, L., Xu, A., & Zhao, J. (2021). Effectiveness of vegetation cover pattern on regulating soil erosion and runoff generation in red soil environment, Southern China. Ecological Indicators, 129, 107956.
Van der Knijff, J. M., Jones, R. J. A., & Montanarella, L. (2000). Soil erosion risk assessment in Europe. Office for Official publications of the European Communities. Pp. 34–35.
Wang, S., Nie, X., Ran, F., Liao, W., Yang, C., Xiao, T., Liu, Y., Liu, Y., & Li, Z. (2023). Human activities control the source of eroded organic carbon in lake sediments over the last 100 years: Evidence from stable isotope fingerprinting. Fundamental Research, 2023, in press.
Yakovenko, V., Kunakh, O., Tutova, H., & Zhukov, O. (2023). Diversity of soils in the Dnipro River valley (based on the example of the Dnipro-Orilsky Nature Reserve). Folia Oecologica, 50(2), 119–133.
Zelenova, V. O., Zelenov, P. V., & Tutova, G. F. (2024). Bioindication potentials of the grass stand and soil macrofauna for assessing the level of anthropogenic transformation of an urban park are complementary. Biosystems Diversity, 32(3), 306–313.
Zhou, P., Luukkanen, O., Tokola, T., & Nieminen, J. (2008). Effect of vegetation cover on soil erosion in a mountainous watershed. Catena, 75(3), 319–325.
Zhukov, O., Yorkina, N., Budakova, V., & Kunakh, O. (2022). Terrain and tree stand effect on the spatial variation of the soil penetration resistance in an Urban Park. International Journal of Environmental Studies, 79(3), 485–501.
Zymaroieva, A., Zhukov, O., Fedonyuk, T., & Pinkin, A. (2019). Application of geographically weighted principal components analysis based on soybean yield spatial variation for agro-ecological zoning of the territory. Agronomy Research, 17(6), 2460–2473.